Development of a physical 2-D model for arc quenching chamber of lightning protection multichamber systems

Chusov A., Podporkin G.
Streamer Electric Company,
Saint-Petersburg, Russia
alexander.chusov@streamer.ru
georgij.podporkin@streamer.ru

Pinchuk M.
Institute for Electrophysics and Electrical Power of the Russian Academy of Sciences,
Saint-Petersburg, Russia
pinchme@mail.ru

Ivanov D., Murashov I., Frolov V.
Peter the Great Saint-Petersburg Polytechnic University, Polytechnicheskaya 29,
Saint-Petersburg, Russia
iuriimurashov@gmail.com,
d.ivanov@list.ru,
frolov.eed@gmail.com

***Abstract*—The multi-chamber systems (MCS) were recently proposed as a prospective lightning protection device. 2D- physical model of arc discharge in MCS discharge chamber was developed in order to perform tests of quenching efficiency for various chamber geometry. It was shown that in case of chamber configuration with hollow electrodes the backflow from electrodes appears at some time instance during the current pulse decay phase.**

Keywords-lightning protection; multi-chamber system; arc discharge; plasma simulations; construction optimization

I. INTRODUCTION

In recent years multi-chamber system (MCS) based arresters have succeeded in lightning protection of overhead power-lines. The example of 'multi-chamber insulator arrester' (MCIA) which combines properties and functions of arrester and insulator [1], is depicted in Fig.1. The MCS consists of a large number of series connected chambers. The example of discharge chamber is given in Fig.2. Each electrode consists of two nested tubes – inner and outer tube. While the outer tube

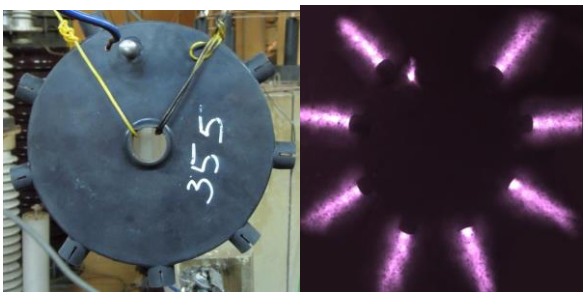

Figure 1. Design of multi-chamber arrester (left) and impulse arc discharge in multi-chamber arrester (right).

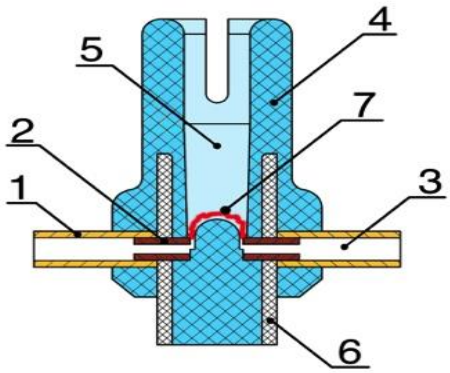

Figure 2. Design of discharge chamber of multi-chamber arrester: 1 – outer tube, 2 – inner tube, 3 – cavity, 4 silicone rubber, 5 – discharge slot, 6 – fiberglass plastic sleeve, 7 – arc.

is constantly copper the material of inner tube can be copper, steel or tungsten [2]. Under the lightning overvoltage electrical breakdown occurs in every single chamber resulting in impulse current flowing through the MCS. Initiated arc discharge causes erosion of the electrode material and chamber wall evaporation due to arc-wall interaction which leads to intensive pressure buildup, plasma outflow and eventually to arc extinction. In numerous experiments performed certain discharge chamber constructions demonstrated enhanced quenching capability. Demonstrated enhanced quenching capability. Optimization of chamber geometry for maximizing of quenching efficiency is one of the most important problem of effective multichamber arrester development. Unfortunately the search for optimal chamber parameters through experiment only is quite difficult, expensive and time consuming. An attempt has been made to develop physical and mathematical

models of the discharge for such systems and calculate parameters in the discharge chamber of arresters [3], [7].

The presented paper describes the development of 2D-physical model of arc discharge chamber and preliminary results of chamber construction optimization.

II. EXPERIMENTAL RESULTS

The discharge in single MCS chamber was investigated experimentally. The experimental setup is described in [4]. The brief review of used diagnostics methods one can find in [5].

A. Current and voltage oscillograms

Oscillograms of current and voltage are shown in Fig. 4 and Fig.6. The 30μF capacitor was used for 10kA current amplitude pulse and 9μF for 3kA. Initial current-rise rate was of 10^9 A/s. The capacitor was charged up to 18-23 kV and then it unloaded on the discharge chamber through the 2 Ohm resistor for 10kA pulse or 6 Ohm for 3kA. Thus, the current amplitude was defined by nominal value of the resistor, the time constant of a discharge circuit was 54 – 60 μs. The energy input into the discharge was of 100 − 200J.

B. Energy deposition measurements

In order to investigate the energy distribution in discharge volume and its variation in time high-speed photographing was executed in narrow spectral range of 550 – 650 nm, limited by optical filters. The spectral emissive ability in the spectral range is linearly proportional to temperature $I_\lambda \sim T$ for estimated plasma temperatures. Assuming that locally deposited energy is spent mostly on gas heating, the optical image reflects a field of energy deposition in the discharge volume [6]. One-dimensional distributions of power density Px(x, t) along the discharge chamber length are depicted in Fig. 5. The graphs indicate the peak value of power density about 130 MW/cm^3 and 200 MW/cm^3

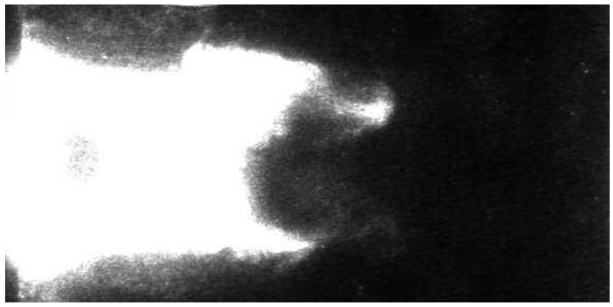

Figure 3. High-speed photo of discharge for current amplitude 10 kA after 10μs

III. DISCHARGE CHAMBER MODEL

The simulation of an impulse arc needs a Multiphysics approach including fluid mechanics, thermal transfer and electrodynamics. The corresponding conservation equations are highly coupled, on the one hand implicitly, because all thermodynamic properties and transport coefficients depend strongly on the temperature, and on the other hand, explicitly, mainly because the flow depends on electromagnetic forces, temperature depends on Joule effects and electric field is linked to the shape and value of the temperature field.

A. General assumptions

In order to simplify the model and emphasize the most important processes involved several assumptions were made:

- The development of outflow is 2D
- The flow is laminar
- The surrounding gas air is at atmospheric pressure
- The plasma is in Local Thermodynamic Equilibrium (LTE), i.e. electron and heavy particles have the same temperature

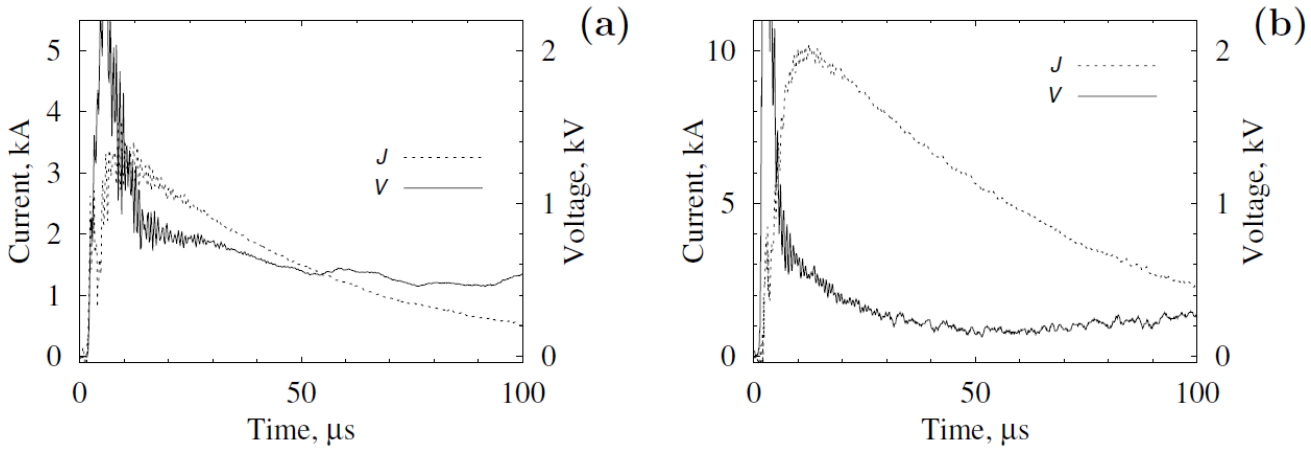

Figure 4. Current (J) and voltage (V) for 10 kA (b) current amplitude test conditions at different time

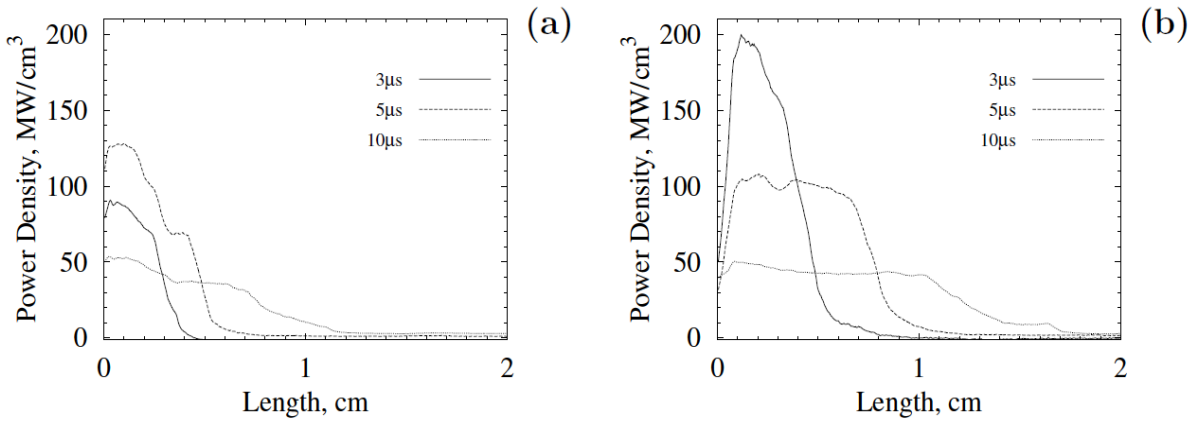

Figure 5. Energy deposition distribution along discharge chamber for 3kA(a) and 10kA(b) current amplitude test conditions at different time

- Thermodynamic properties only depend on temperature
- The influence of magnetic forces and arc radiation was neglected
- The influence of electrode erosion and material ablation is taken into account only through modification of thermodynamic properties temperature dependence
- The flow is laminar

This makes it possible to treat the plasma as a single fluid. Balance equations can then be used for mass, momentum and energy.

$$\frac{\partial \rho}{\partial t} + \nabla \cdot (\rho \vec{v}) = 0 \qquad (1)$$

$$\frac{\partial \rho \vec{v}}{\partial t} + \nabla \cdot (\rho \vec{v}\vec{v}) = -\nabla p + \mu \Delta \vec{v} \qquad (2)$$

$$\frac{\partial \rho H}{\partial t} + \nabla \cdot (\rho \vec{v} H) = \frac{\partial p}{\partial t} + \nabla \cdot \lambda \nabla T + \vec{v} \cdot \nabla p + Q \qquad (3)$$

Above we denote with ρ the density, v the velocity, p the pressure, H the internal energy, λ the thermal diffusivity, μ the viscosity. The last term Q corresponds to Joule heating. It was assumed that power density curve has the same shape as 8/50 µs current impulse. Double exponential impulse was taken to model it:

$$I(t) = \frac{I_{max}}{\eta} * (e^{-\frac{t}{\tau_1}} - e^{-\frac{t}{\tau_2}}) \qquad (4)$$

τ_1 = 2 µs – current pulse rise time

τ_2 = 70 µs – current pulse decay time

I_{max} – current peak value

η – correction factor

B. Thermodynamic properties

In order to solve governing equations (1)-(3) it is necessary to set thermal diffusivity λ, specific heat C_p and viscosity μ as functions of temperature. For this purpose the composition and thermodynamic properties of discharge were calculated using LTE assumption. The discharge was treated like a mixture of air plasma and products of electrodes erosion and chamber wall vaporization. The chamber wall material is silicone rubber while electrodes are made of copper and tungsten. Method of plasma composition and thermodynamic properties calculation is described in [3]. The following species were considered:

- monoatomic species (22 species): e, O, O^+, O^{2+}, O^-, C, C^+, C^{2+}, C, H, H^+, H^-, Si, Si^+, Si^{2+}, N, N^+, N^{2+}; S, S^+, S^{2+}, S^-;
- diatomic species (36 species): O_2, O_2^+, O_2^-, C_2, C_2^+, C_2^-, CO, CO^+, H_2, H^{2+}, H^{2-}, OH, OH^+, CH, CH^+, Si_2, SiO, SiH, SiC, N_2, N_2^+, N_2^-, CN, CN^+, CN^-, NH, NH^+, NO, NO^+, NO^-, S_2, S_2^-, SO, SO^-, SH, SH^-;

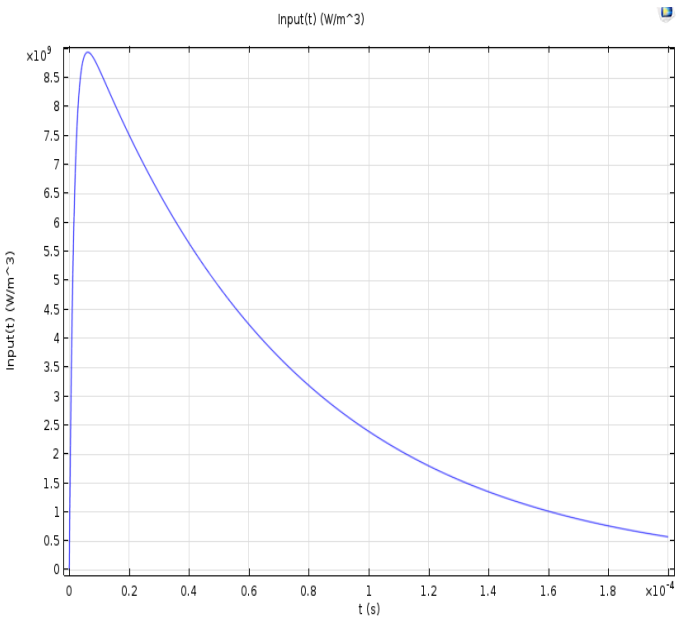

Figure 6. Joule heating power density

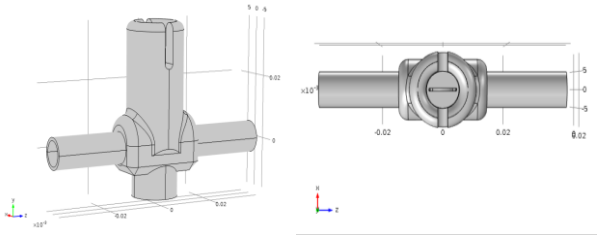

Figure 7. Discharge chamber 3D-model: Left-general view, Right – Top View.

- polyatomic species (55 species): O_3, C_3, C_4, CO_2,C_2O, C_3O_2, H_2O,H_2O_2 , CH_2, CH_3, CH_4, C_2H, C_2H_2, C_2H_4, C_2H_6, HCO, H_2CO, Si_3, SiH_2, SiH_3, SiH_4, SiC_2, Si_2C, CN_2, C_2N, C_2N_2, H_2N, H_2N_2, H_3N, H_4N_2, NO_2, NO_2^-, NO_3, N_2C, N_2O, N_2O^+, N_2O_3, N_2O_4, N_2O_5, N_3, HNO, HNO_2, HNO_3, CHN, CHNO, CNO, S_3, S_4, S_5, S_6, SO_2, SO_2^-, SO_3, S_2O, H_2S.

The calculated composition of plasma allows to calculate its thermodynamic properties, in particular, thermal conductivity and specific heat capacity which determines the heat transfer along the discharge channel. All the quantities are calculated in temperature interval from 300 K to 60000 K.

C. Computational domain

The 3D-model of discharge chamber (see Fig.7) shows no axial symmetry but discharge itself is initiated and developed in a narrow rectangular shaped volume (discharge volume) bounded by silicone walls. The width of the discharge volume (slot width) is much smaller than its length thus it was decided to simulate plasma flow as two-dimensional (as it was pointed in general assumptions). In order to acquire 2D-computational domain the vertical cross-section of discharge chamber was built and then extruded along normal by the distance equal to width of the nozzle slit. Eventually constructed 2D-domain is depicted in Fig.8.

D. Use of COMSOL Multiphysics

Previously described mathematical model (4) is implemented in COMSOL software using the governing equations of the following models:

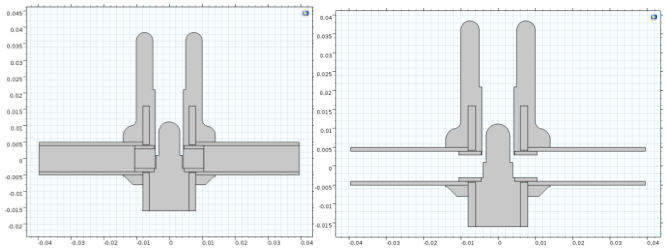

Figure 9. Discharge chamber with solid (left) and hollow (right) electrodes

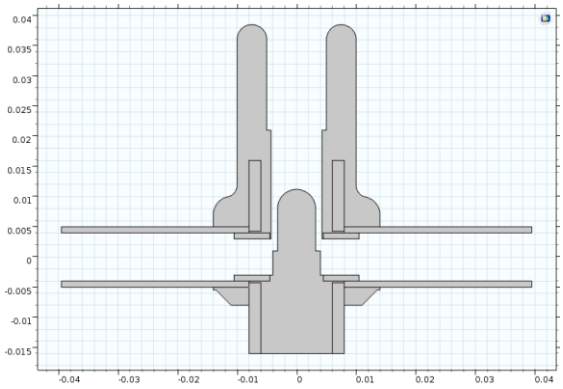

Figure 8. 2D-computational domain in COMSOL Multiphysics

- Weakly Compressible Navier-Stokes Equation (Laminar Flow Module);
- Heat Transfer in Fluids (Heat Transfer Module);

The specific thermodynamic properties (mass density, specific heat), transport coefficients (thermal and electrical conductivity, viscosity) of discharge are all temperature dependent and are previously calculated. As was mentioned, these equations are highly coupled and a careful attention is necessary to initiate calculation and to reach convergence. Due to strong nonlinearity of heating source function (see Fig.6) special attention should be taken to magnitude of input heat density which in reality is defined by current level.

IV. RESULTS AND DISCUSSIONS

The first evaluation of developed 2D discharge model simulations were performed for two chamber constructions with only difference in electrode structure: the first one is made with solid electrodes while the second one has hollow electrodes (see Fig.9). The simulation is started with uniform temperature and density distributions, the initial pressure is set to 1 atm. The full simulation and lasts for 200 μs (lightning pulse phase duration).

A. Gas flow in discharge chamber

First calculation attempts were performed for energy input corresponding to moderate impulse currents of magnitude 3 kA (see Fig.64 (b)). To find out which chamber provides the most intensive outflow the time variation of maximum flow velocity over the whole domain was calculated for both chambers. It can be seen from the Fig.13 and Fig.14 that gas flows out a little bit faster for case of chamber with solid electrodes. The deeper insight into flow process can be provided by analysis of velocity spatial distributions for different time instants. Calculated distribution at time of 20 μs is depicted on Fig.10. Colors on the color bar next to diagram correspond to velocity magnitude in m/s. To validate calculated velocity it was compared with results of plasma jet high-imaging conducted for single chamber (See Fig.11) Five frames of plasma flow with time interval of 20 μs are depicted on Fig. 12. arranged in a

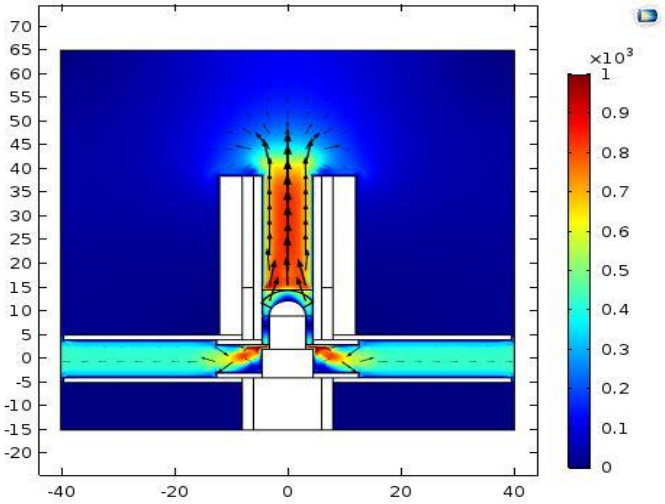

Figure 10. Flow velocity distribution. The units for color bar numbers are m/s

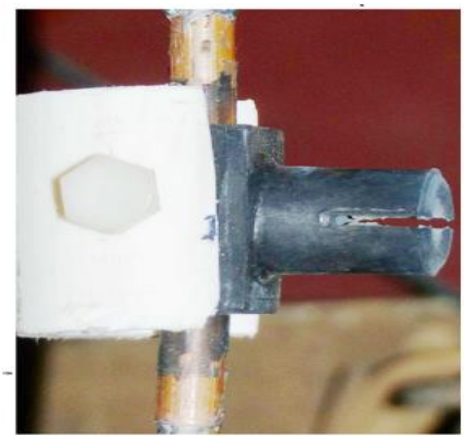
Figure 11. Maximum outflow velocity: hollow electrodes

column. The velocity of flow for each frame was calculated as division of flow shift (defined by difference of blue bar position) by time difference. It can be seen that at 20 μs the velocity is 1100 m/s while the calculated value is about 1000 m/s which seems to be quite a good matching. Fast heating of gas in discharge gap during the current rise stage (first 8 μs) causes gas to flow tube out of the chamber with high speed. The inner region of electrode bounded (electrode volume) is filled with gas and the inflow keeps on going due to continuing heating. The flow passes through the narrow gap between electrode tube and silicone wall which forms an outlet channel for hot gas flowing out from discharge volume. To investigate the flow dynamics in this transition zone the velocity was calculated at fixed point. The location of transition zone (area bounded by red circle) and the fixed point are depicted in Fig.15. The graph on Fig.16 reflects the evolution of velocity in time. At 150 μs the flow velocity goes to zero i.e. the flow reverses its direction. The diagrams of flow velocity and heat flux for initial stage of flow development (~20 μs) and in the late decay stage (~200 μs) are depicted in Fig.17 and Fig.18 respectively. The arrows represent direction of velocity/heat flux while the size is proportional to quantities amplitude.
The comparison of diagrams allows to see the global change of flows behavior: firstly strong heat flux propagates in the direction of electrode volume and later it passes transition zone pointing inwards.

B. Discussions

Initial simulation of impulse discharge in MCS chamber allowed to compare the gas flow in discharge chambers with

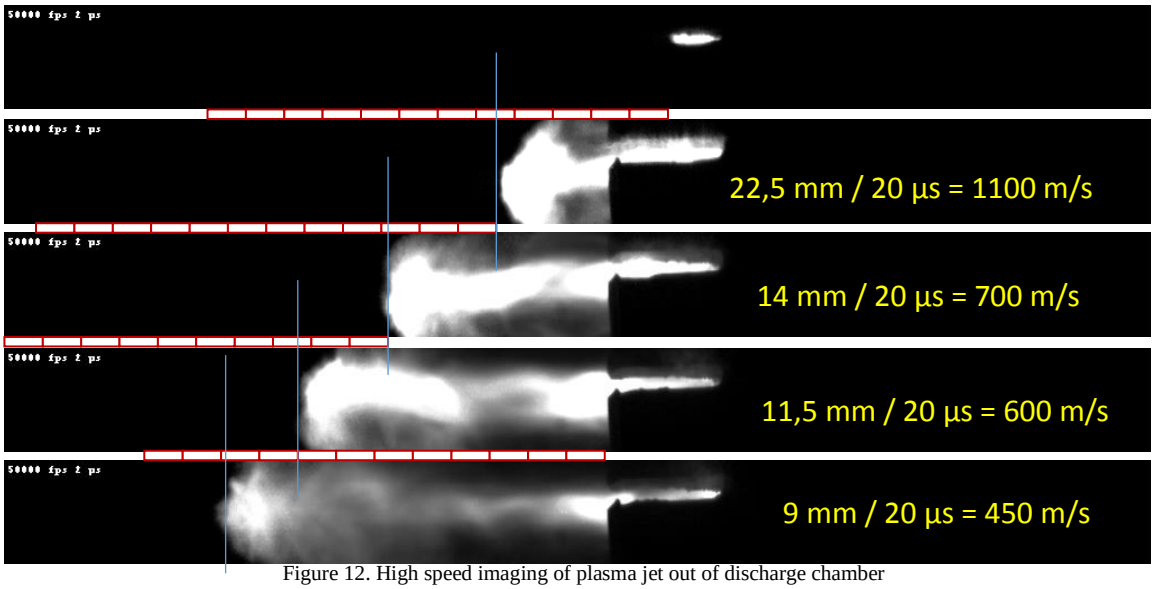

Figure 12. High speed imaging of plasma jet out of discharge chamber

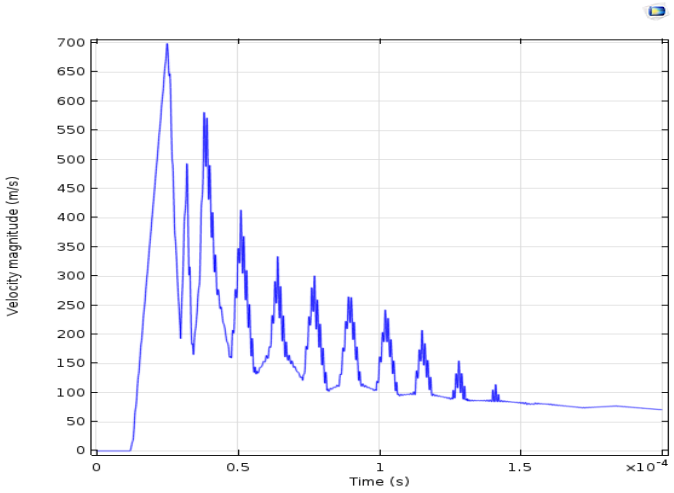

Figure 13. Transition zone (marked by red circle). The depicted blue point is set for velocity calculation

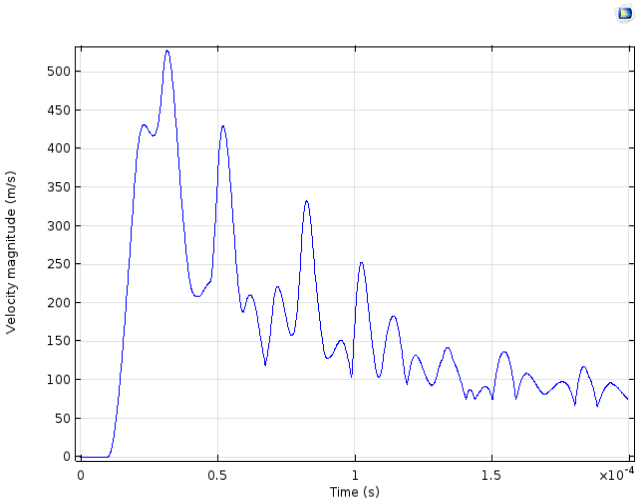

Figure 14. Transition zone (marked by red circle). The depicted blue point is set for velocity calculation

solid and hollow electrodes. It comes out that gas flow is more intensive for case of solid electrodes. The higher velocity of outflow is supposed to increase quenching capability meaning that from this point of view the solid electrodes are preferable. However the following analysis helped to observe the formation of after-pulse flow directed outwards from the discharge chamber. This additional backflow from hollow electrodes seems to be a positive feature because it can lead to increase of density in discharge volume after impulse current phase (what is believed to decrease the conductivity of residual arc channel) and provide additional cooling of electrode surface.

V. CONCLUTIONS

The MCS discharge chamber 2D-model was successfully developed and implemented using COMSOL Multiphysics software. In its current state the model can already produce qualitative results which can be used in development process. Particularly simulations performed for chamber construction with nested electrodes allowed to visualize the formation of additional backflow from hollow electrode what is expected to be a positive feature and lead to quenching efficiency enhancement. Further work will be needed on electrode sheaths, material properties and the ignition process to get accurate qualitative results.

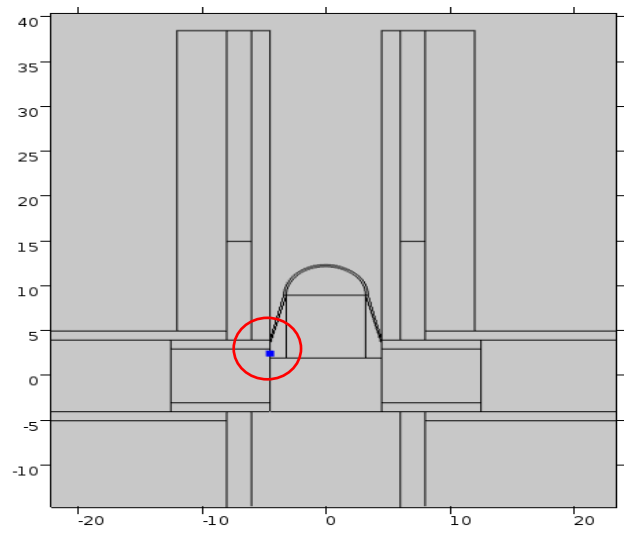

Figure 15. Transition zone (marked by red circle). The depicted blue point is set for velocity calculation

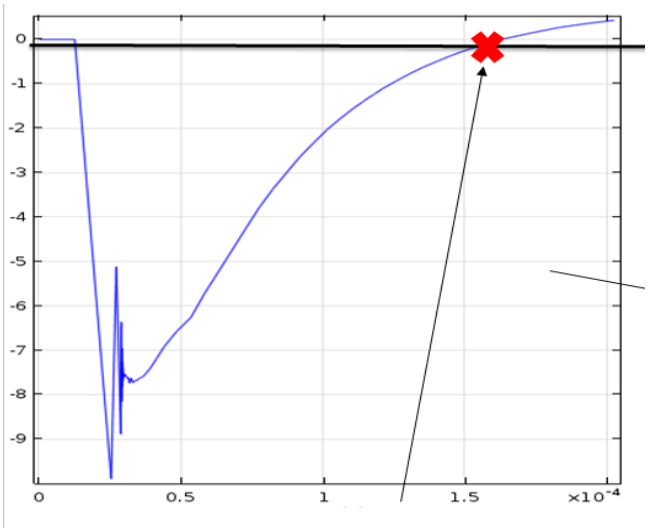

Figure 16. The flow velocity at fixed point inside electrode tube. Red cross indicates the moment of flow reversal

VI. REFERENCES

[1] G.V. Podporkin, V.E. Pilshikov, E. S. Kalakutsky, Alexander D. Sivaev, E.Yu.Enkin "Development of multi-chamber arrester-insulator for lightning protection of 220 kV overhead transmission lines".

[2] Podporkin G., Enkin E., Pilshikov V., Zhitinev V. "Lightning protection of overhead distribution linesmulti-chamber insulator-arrester of a novel design", CIGRE SC C4 2012 Hakodate Colloq.

[3] Frolov V. Y., Ivanov D. V., Murashov Y .V. ,Sivaev A D "Calculation of the composition of of plasma of an arc pulsed discharge in a multichamber arrester" 2015 Technical Physics Letters 41 310–313.

[4] Budin A, Pinchuk M, Pilschikov V, Leks A and Leont'ev V "Experimental stand for investigations of protective device for overhead power lines" 2016 Instruments and Experimental Techniques

[5] Pinchuk M, Bogomaz A, Budin A and Rutberg P "Electrode plasma jets in powerful pulsed discharge in high-pressure gas" 2014 Plasma Science, IEEE Transactions on 42 2434–2435

[6] Pinchuk M., Bogomaz A., Budin A, Kumkova I.,Sivaev A.,Chusov A.,Zaynalov R. "Energy deposition in discharge chamber of lightning protection multichamber system" 2016 Technical Physics Letters (in print)

[7] Kozakov R., Khakpour A.,Gorchakov S.,Uhrlandt D.,Ivanov D.,Murashov I., Podporkin G., Frolov V. "Investigation of a multi-chamber system for lightning protection at overhead power lines" XXI symposium on physics of switching arc

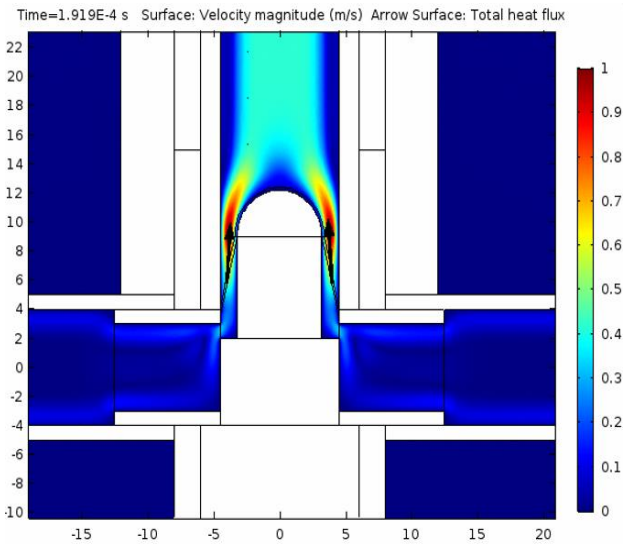

Figure 17. The diagram of flow velocity for t=19.2 μs. The arrows point to the direction of heat flux. The arrow size is proportional to heat flux magnitude

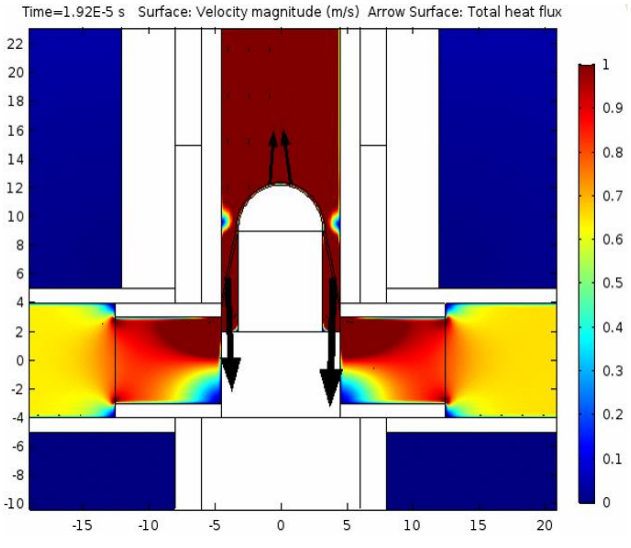

Figure 18. The diagram of flow velocity for t=192 μs. The arrows point to the direction of heat flux. The arrow size is proportional to heat flux magnitude